Forelimb unloading impairs glenohumeral muscle development in growing rats

Sophia K. Tushak[a,1], Margaret K. Tamburro[a,1], Emily B. Fawcett[a], Lauren E. Merritt LE[b], Katherine R. Saul[b], PhD, and Jacqueline H. Cole[a,*], PhD

[1] These authors contributed equally to this work.

[a] Joint Department of Biomedical Engineering, University of North Carolina, Chapel Hill, NC, and North Carolina State University, Raleigh, NC, USA

[b] Mechanical and Aerospace Engineering, North Carolina State University, Raleigh, NC, USA

***Corresponding author:**
Dr. Jacqueline H. Cole, PhD
Assistant Professor
North Carolina State University & University of North Carolina-Chapel Hill
4212B Engineering Building III
911 Oval Drive
Campus Box 7115
Raleigh, NC 27695-7115
Telephone: 919-515-5955
Email: jacquecole@ncsu.edu

Abstract

Proper joint loading is essential for healthy musculoskeletal development. Many pediatric neuromuscular disorders cause irreversible muscle impairments resulting from both physiological changes and mechanical unloading of the joint. While previous studies have examined the effects of hindlimb unloading on musculoskeletal development in the lower limb, none have examined solely forelimb unloading. Thus, a large deficit in knowledge of the effect of upper limb unloading exists and must be addressed in order to better understand how the glenohumeral joint adapts during development. Two forelimb unloading models were developed to study the effects of varying degrees of unloading on the glenohumeral joint in growing rats: forelimb suspension (n=6, intervention 21 days post-natal) with complete unloading of both limbs via a novel suspension system and forearm amputation (n=8, intervention 3-6 days post-natal) with decreased loading and limb use in one limb after below-elbow amputation. After 8 weeks of unloading, changes in muscle architecture and composition were examined in ten muscles surrounding the shoulder. Results were compared to control rats from a previous study (n=8). Both methods of altered loading significantly affected muscle mass, sarcomere length, and optimal muscle length compared to control rats, with the biceps long head and triceps long head observing the most marked differences. Forearm amputation also significantly affected muscle mass, sarcomere length, and optimal muscle length in the affected limb relative to the contralateral limb. Muscle composition, assessed by collagen content, remained unchanged in all groups. This study demonstrated that forearm amputation, which was administered closer to birth, had greater effects on muscle than forelimb suspension, which was administered a few weeks later than amputation.

Introduction

Mechanical loading is critically important for healthy musculoskeletal development[1,2] and maintenance[3,4]. In adult murine models, unloading via hindlimb suspension, microgravity during spaceflight, and muscle paralysis causes changes in muscle architecture. For example, unloading in adult murine animals caused substantial reductions of 41-66% in skeletal muscle size, mass, and strength[6,8,9], as well as up to 13% longer sarcomere lengths[8]. However, muscle composition measured by collagen content was unaffected by unloading in adult rodents[7,11]. In growing animals, unloading is particularly impactful, causing irreversible musculoskeletal changes[5,12,56], including altered joint morphology[12], which influences surrounding muscle, and decreased muscle mass by over 3 to 5-fold[5,56]. However, the effects of unloading on other muscle architecture metrics (e.g., sarcomere length, optimal muscle length) and muscle composition (e.g., collagen content) have not previously been examined in growing animals.

Unloading models have traditionally focused on the hindlimbs[15], resulting in limited understanding of the specific contributions of forelimb unloading to changes in muscle of glenohumeral joint, particularly during development. With a combined incidence of more than 5 per 1,000 live births[16–19], pathologies affecting the developing muscles surrounding the glenohumeral joint (e.g., brachial plexus birth injury[20–22], congenital muscular dystrophy[23–25], cerebral palsy[26–28], and congenital myasthenia gravis[29–31]) have substantial implications for the effects of altered forelimb loading during development. However, isolating the role that altered loading plays in these conditions is challenging, since, for example, nerve injury also directly contributes to detrimental muscle[12,13] changes. Hence, the independent contributions of altered mechanical loading and nerve injury or other congenital changes to musculoskeletal development following neuromuscular disorders and injuries are difficult to elucidate. Understanding the contributions of unloading to these pathologies is an important step in determining which changes

result directly from injury or disease and which are a functional consequence of altered joint loading, which may aid treatment development to restore muscle function.

Because of anatomical similarities to human shoulders[32,33] and rapid development to skeletal maturity[34], murine models are often used to study these injuries and diseases[20–31]. While murine hindlimb unloading[35] and partial unloading paradigms exist[36], to date no study has implemented a partial or complete forelimb unloading paradigm that targets the glenohumeral joint during neonatal development. A previous mouse model of bipedal locomotion training to improve function following spinal cord injury involved forelimb unloading, although these effects were not evaluated, and the animal was placed in an unnaturally upright posture, making this model unsuitable for studying long-term forelimb unloading[37]. We implemented two novel murine models to simulate variable degrees of mechanical unloading in the glenohumeral joint that occurs with this array of neuromuscular diseases and injuries: forelimb suspension and forearm amputation. Our objective was to determine the effect of these forelimb unloading models on the postnatal development of muscles surrounding the glenohumeral joint, in particular muscle architecture and composition.

Methods

All procedures were approved by the Institutional Animal Care and Use Committee at North Carolina State University prior to the start of the study. Male and female Sprague Dawley rats (Charles River Laboratories, Wilmington, MA) were subjected to forelimb unloading using one of two different methods (Fig. 1): forelimb suspension (n = 6) or forearm amputation (n = 8). Results from the unloading groups were compared to results from a control group (n = 8).

Forelimb Suspension

Six Sprague Dawley rats (2 female, 4 male) from three litters were exposed to forelimb unloading promptly after weaning at 3 weeks of age. Rats were placed in fitted harnesses, connected to a custom suspension system, and subjected to a six-week period of continuous unloading in both forelimbs (Fig. 2). Details of our suspension system were described previously[38]. The rats experienced a 12-hour light/12-hour dark cycle. Rat chow (Purina, Woodstock, Ontario, Canada) and HydroGel® (ClearH2O®, Inc., Westbrook, ME) were offered *ad libitum*. HydroGel® was used instead of water, because the typical water bottle interfered with the suspension system. At 9 weeks of age and after six weeks of loading, the rats were euthanized with CO_2 inhalation followed by bilateral thoracotomy.

Forearm Amputation

Eight Sprague Dawley rat pups (2 female, 6 male) from the same three litters as the forelimb suspension group received forearm amputations at 3-6 days of age. Rat pups were anesthetized with isoflurane, and right forearms were amputated through elbow disarticulation using aseptic technique, with the contralateral forelimbs remaining intact. The wound was irrigated and closed with tissue adhesive and suture. To minimize pain, rats received a local anesthetic (bupivacaine) at the incision site during surgery, one dose of buprenorphine (0.01 mg/kg) and carprofen (5 mg/kg) immediately after surgery, and a course of carprofen once per day for five days after surgery. Upon recovery from anesthesia, rat pups were returned to their dams and regularly monitored for signs of acceptance. Rat pups were weaned from their dams at 3 weeks of age and housed three per cage in the same room with the same accommodations as the forelimb

92 suspension group, except they were given a typical water bottle. At 8 weeks of age, the rats were
93 euthanized with CO_2 inhalation followed by bilateral thoracotomy.
94
95 *Control*
96 Control comparison data were obtained from previously assessed rats that underwent a
97 sham surgery[50]. In that study, 8 Sprague Dawley rat pups (3 female, 5 male) from three litters
98 received sham surgeries at 3-6 days of age that exposed the brachial plexus nerve bundle through
99 the right pectoralis major, but no subsequent nerve injury was administered, and the contralateral
100 forelimbs were kept intact. The wound was irrigated and closed with tissue adhesive. To minimize
101 pain, one dose each of buprenorphine and carprofen was administered immediately following
102 surgery. Rats received the same post-surgical care as the forearm amputation group. At 8 weeks
103 of age, the rats were euthanized with CO_2 inhalation followed by bilateral thoracotomy. For the
104 control group, the left forelimb – which did not undergo surgery – was considered unaffected and
105 used for comparison to the unloading groups.
106
107 *Muscle Dissection*
108 Following euthanasia, the upper body was harvested using a guillotine to remove both the
109 head and lower body. The torso was then fixed in 10% neutral buffered formalin for two days and
110 stored in 70% ethanol at 4°C until muscle dissection. In 11 rats (5 control, 3 suspension, 3
111 amputation), 10 muscles surrounding the shoulder and upper forelimb were dissected bilaterally
112 and stored in 70% ethanol at 4°C until architecture analysis: pectoralis major, acromiodeltoid,
113 spinodeltoid, biceps long head, biceps short head, subscapularis, supraspinatus, infraspinatus, teres
114 major, and triceps long head[39]. In the remaining 11 rats (3 control, 3 suspension, 5 amputation),

four muscles (biceps long head, biceps short head, upper and lower subscapularis) were harvested bilaterally for composition analysis. The proximal end of each muscle was embedded in optimum cutting temperature compound and set in 2-methylbutane cooled by liquid nitrogen, and the entire muscle was then snap frozen and stored at -80°C until sectioning.

Optimal Muscle Length

Muscle mass and muscle length were measured for the muscles stored at 4°C. After blotting excess ethanol, muscles were weighed on a digital scale (resolution of 0.01 g). For each muscle, 9 muscle fibers were extracted, 3 each from the proximal, middle, and distal regions of the muscle. Sarcomere lengths were measured via a 5.0-mW HeNe laser with a wavelength of 633 nm (Thorlabs, Newton, NJ) using an established laser diffraction method[26]. All muscle lengths and distances between each diffraction band were measured using digital calipers (resolution of 0.01 mm). The 9 sarcomere measurements were averaged to find the mean sarcomere length for each muscle. To determine the excursion capacity of the muscles and account for possible stretch in the fixed muscle as indicated by sarcomere length, optimal muscle length was calculated[40]:

$$L_0^m = L^m \left(\frac{2.4\ \mu m}{L^s} \right)$$

where L^m is muscle length and L^s is sarcomere length. The optimal sarcomere length corresponded to that of rat skeletal muscle (2.4 µm).

Muscle Fibrosis

In muscles stored at -80°C, three transverse cryosections with a thickness of 10 µm were obtained from each muscle (Cryotome FSE Cryostat, Thermo Scientific, Halethorpe, MD), mounted to a silanized slide, and stored at -80°C prior to staining. Muscle sections were stained

with Masson's trichrome (American MasterTech, Lodi, CA) to identify collagen I deposition, a measure of fibrosis and muscle stiffening, and imaged at 20X magnification with light microscopy (EVOS® FL Cell Imaging System, Thermo Scientific, Halethorpe, MD) In three sections per muscle, collagen content was calculated as the ratio of collagen area to muscle tissue area using a custom image processing protocol (MATLAB®, The MathWorks, Inc., Natick, MA).

Statistical Analyses

To verify whether side-to-side differences were insignificant for the forelimb suspension and control groups (as expected) and to identify whether differences existed in muscle metrics between the affected and unaffected forelimbs for the amputation group, paired t-tests were used. Muscle architecture (mass, sarcomere length, optimal muscle length) and composition (collagen content) metrics were compared across the three groups (control, forelimb suspension, forearm amputation) using one-way ANOVA with Tukey's post-hoc tests. For the group comparisons, data from only one forelimb was used: right for both unloading groups and left (unoperated) for the control group. All analyses were performed in RStudio Cloud (v. alpha, The R Foundation for Statistical Computing, Vienna, Austria) with a significance level of $\alpha = 0.05$.

Results

Side Differences Within Each Group

In the control and forelimb suspension groups, no significant side-to-side differences were found for any of the metrics, apart from the pectoralis major muscle mass in the control group, which was lower in the sham limb (right) compared to the unimpaired limb (left) as previously reported[39]. This was expected, because the sham surgery involved a transverse infraclavicular

161 incision through the pectoralis major to expose the brachial plexus. In the forearm amputation
162 group, muscle mass was an average of 37.7% lower for muscles in the right (affected) limb
163 compared to the left (unaffected) limb (Table 1). Affected limb muscle mass was significantly
164 lower than unaffected for acromiodeltoid (18.1 ± 1.7%, p = 0.0153), biceps long head (54.9 ±
165 7.9%, p = 0.0136), and triceps long head (56.8 ± 6.0%, p = 0.0136).

166 In the forearm amputation group, sarcomere length was not different between limbs for
167 most muscles. Sarcomeres were significantly longer in the affected biceps long head (17.6 ± 1.3%,
168 p = 0.0005) compared to unaffected muscles (Table 1). However, on average optimal muscle
169 lengths were an average of 22.7% shorter in muscles of the affected limb compared to the
170 unaffected limb. Optimal muscle lengths were significantly shorter in affected acromiodeltoid
171 (27.1 ± 3.9%, p = 0.010) and biceps long head (39.6 ± 3.1%, p = 0.0002) compared to the
172 unaffected side.

173 Collagen content, indicative of muscle fibrosis, did not differ significantly between left and
174 right limbs in any group.

175

176 *Group Differences*

177 Muscle mass differed significantly across groups for biceps long head and triceps long head
178 (Fig. 3, Table 1). Compared to the control group, the forearm amputation group had significantly
179 lower average muscle mass in the biceps long head (51.0%, p = 0.0202) and triceps long head
180 (57.7%, p = 0.0229). Similarly, compared to the suspension group, the amputation group had lower
181 average muscle mass in the biceps long head (51.6%, p=0.0202) and triceps long head (56.9%, p
182 = 0.0437). No significant differences in muscle mass were found between the forelimb suspension
183 and control groups.

Group differences were also observed in sarcomere length for acromiodeltoid, spinodeltoid, biceps long head, subscapularis, supraspinatus, and teres major (Fig. 4, Table 1). Compared to the control group, the amputation group had, on average, significantly shorter sarcomeres in the acromiodeltoid (10.9%, $p = 0.0235$) and subscapularis (10.4%, $p = 0.0377$) muscles but longer sarcomeres in spinodeltoid (12.6%, $p = 0.000612$) and teres major (25.7%, $p = 0.0000366$). Compared to those in the suspension group, average sarcomere length in the amputation group was significantly longer in biceps long head (17.4%, $p=0.000300$) and teres major (9.2%, $p = 0.00212$). Compared to control, the suspension group had significantly shorter sarcomeres in the biceps long head (8.5%, $p=0.0449$), subscapularis (13.5%, $p = 0.0102$), and supraspinatus (14.6%, $p = 0.0401$) muscles but longer sarcomeres in spinodeltoid (8.3%, $p = 0.00792$) and teres major (15.1%, $p = 0.00148$).

Optimal muscle length differed by group for biceps long head, biceps short head, and triceps long head (Fig. 5, Table 1). Compared to control, average optimal muscle length in the amputation group was significantly shorter for biceps long head (30.1%, $p = 0.0145$) and triceps long head (28.1%, $p = 0.00185$), indicating reduced longitudinal growth. Similarly, compared to suspension, average optimal muscle lengths in the amputation group were significantly shorter for biceps long head (36.9%, $p = 0.00493$), biceps short head (27.0%, $p = 0.0273$), and triceps long head (35.8%, $p=0.000372$).

Qualitative analysis of histologic images revealed minimal differences across the groups in collagen staining for the 4 analyzed muscles (biceps long head, biceps short head, upper and lower subscapularis muscles) (Fig. 6). Quantitative analysis of these images showed that the ratio of collagen area to total muscle area did not differ significantly across the three groups for any of the 4 muscles examined (Table 2).

Discussion

Unloading with the two models had different effects on the growth of forelimb muscles. The suspension group did not affect muscle mass oroptimal muscle lengths relative to control, except for an increased optimal length for biceps short head. In contrast, the amputation intervention led to lower muscle mass and optimal muscle length for several muscles in the affected forelimb compared to the contralateral limb, suggesting that unloading via forearm amputation during postnatal development can inhibit muscle growth. Specifically, muscle mass was lower in the acromiodeltoid, biceps long head, and triceps long head, and optimal muscle length was shorter in the acromiodeltoid and biceps long head following amputation. The amputated group also had lower muscle mass and shorter optimal muscle length in the affected limb compared to the forelimb suspension (right affected limb) and control (unaffected limb) groups. On average, the amputated biceps and triceps long head muscles were approximately half the mass and 75% of the optimal length of the corresponding muscles in the suspended and control groups.

The amputation procedure provides an explanation for the specific affected muscles in this group. The biceps long head, biceps short head, and triceps long head originate at the scapula and insert to the proximal radius or ulna. During the amputation procedure, the severing at the insertion point releases the muscles and causes widespread denervation and atrophy, leading to reduced muscle mass[52]. In other studies found that denervated extensor digitorum longus muscle mass in growing rats increased after initial atrophy, following similar growth patterns as the control contralateral limbs, but soleus muscle mass decreased relative to the control[53]. The authors suggested that the increased growth was due to elevated protein synthesis after continued

lengthening of the muscle, while the decrease in growth was attributed to a reduction in protein synthesis after continued shortening of the muscle. Although the biceps short head was denervated, it likely experienced extended periods of lengthening, causing it to grow similar to the suspension and control groups. The biceps and triceps likely experienced shortening over the duration of the study due to the release at amputation, which contributed to muscle mass loss and shortening. The other forelimb muscles were not affected by the amputation procedure and therefore there was no marked differences in muscle architecture.

The suspension group also exhibited changes in muscle architecture relative to the control group, which may be explained by the relative immobilization of the limbs. For example, immobilization in innervated lower limb muscles in growing rats found that a decrease in muscle mass compared to a control was attributed to higher levels of protein breakdown and reduced protein synthesis in the affected muscles when the muscles were held in a shortened position[54]. When held in a lengthened position, immobilized muscles in the lower limbs of growing rats exhibited slightly increased muscle mass compared to the control, which was attributed to decreased protein breakdown and increased protein synthesis during active and passive activity of the muscles[54]. The rats in the suspension group, although immobilized in the upper limbs, experienced typical muscle activity as seen in control rats while performing daily eating and cleaning activities, so muscle mass was not significantly affected by limb unloading because rats had full mobility of the unloaded limbs.

Altered loading had a broader and more varied impact on sarcomere length. Within the amputation group, the biceps long head had shortened optimal length but longer sarcomere length on the affected side compared to the unaffected side. The suspension and amputation groups exhibited similar changes in muscle sarcomere length across the different muscles, with shorter

253 sarcomeres in subscapularis, and longer sarcomeres in spinodeltoid and teres major, compared to
254 control, with additional varied effects in the acromiodeltoid and biceps long head. Hindlimb
255 unloading has been shown to reduce titin density in the adult female rat soleus and plantaris
256 muscles[55]. Since titin plays an integral part in sarcomere positional stability, significant losses in
257 titin composition causes vast changes in contractile activity and likely force production. Sarcomere
258 length contributes to optimal muscle length and muscle force production. Any deviation from the
259 optimal sarcomere length causes actin and myosin to inefficiently interact, which limits force
260 production in the muscle. Force production in a muscle-tendon unit, however, is not only governed
261 by muscle length; cross-sectional area is directly proportional to the amount of force each muscle
262 can harvest[49] and is likely affected by changes in muscle mass[51]. Although sarcomere lengths for
263 the anteriodeltoid, spinodeltoid, subscapularis, supraspinatus, and teres major were markedly
264 different in the unloading groups, optimal muscle lengths for these muscles remained the same
265 compared to the control group. Since optimal muscle length is a ratio of sarcomere length to
266 measured muscle length, the unchanged optimal muscle length across groups is likely due to
267 similar changes in sarcomere and optimal muscle lengths. Based on this, the biceps long head and
268 triceps long head, which displayed remarkably lower muscle mass and longer sarcomere lengths
269 that translated to shorter optimal muscle lengths, experienced the greatest decrease in muscle-
270 tendon force production across the board.

271 These results are consistent with a previous study that investigated changes in muscle
272 architecture in growing rats after neonatal injury to the brachial plexus nerve[51]. When comparing
273 the affected limb to the contralateral limb, muscle mass in the same ten muscles as in this study
274 was significantly less in all but one observed muscle, including the biceps long head and triceps
275 long head, similar to the amputation group in this study. Concurrent to the previous study,

sarcomeres in the amputation group were significantly longer in the teres major and biceps long head, along with the teres major in the suspension group relative to the control group. Unlike the injury groups, the suspension group, however, did exhibit shorter sarcomeres in the biceps long head compared to the control group. This comparison shows that muscle mass and sarcomere length in the amputation group more closely mimicked those of injury groups seen in the literature. Optimal muscle length was shorter in the biceps long head for both unloading groups, and biceps short head for the suspension group, which showed that the suspension group more closely resembled the injury groups seen in literature. The triceps long head was significantly affected by both unloading methods, but not by nerve injury, which could mean that the triceps long head muscle length is more sensitive to changes in loading than denervation.

Altered loading did not have a significant impact on muscle collagen content, with similar amounts of fibrosis between limbs, as well as across the amputation, suspension, and control groups. These findings are consistent with previous studies in adult female rat soleus muscle after 2 weeks of hindlimb unloading via tail-casting[11]. Although muscle fibrosis has been observed in children with neuromuscular disorders like cerebral palsy[42] and with nerve injury[43,51], our results indicate that fibrosis is unlikely to result as a consequence of reduced loading, and may instead result from other factors such as direct tissue injury or other physiological consequence..

Results from previous unloading studies vary, depending on animal age and method of unloading. Aprevious study investigating the effects of zero gravity on muscle in 3-month old mice found that mass in three leg muscles were not significantly affected by 30 days in space where observed grooming rate was high[9]. Since the mice maintained daily grooming activity, the muscles were activated throughout unloading, and these results are similar to our forelimb unloading condition with limited muscle effects. Previous hindlimb unloading studies reported muscle

atrophy and decreased muscle mass. One study examined the effect of 30-day space flight on 19-week old mice and found that hindlimb muscle mass was not significantly affected by weightlessness but trended towards decreased soleus and extensor digitorum longus mass in the unloading groups[9]. This could be close to the cut-off of growing and adult. Another study using a tail-casting hindlimb unloading model in young adult female rats found that the addition of combined isometric, concentric, and eccentric muscle stimulation dampened muscle mass loss compared to the untrained contralateral limb, and muscle mass was unchanged from the regular weight-bearing group[44]. This could help adult rats maintain their muscle mass during unloading. In a partial weight-bearing study, 10-week old adult female mice gastrocnemius muscle was found to be significantly lower mass than that of the control groups[36]. Another hindlimb unloading study with adult male rats found that soleus, plantaris, adductor longus, gastrocnemius, and tibialis anterior muscle mass was significantly reduced after hindlimb unloading compared to typical weight-bearing. Isometric exercise attenuated the effects of unloading in the soleus by 54%. Isometric exercise, however, did not aid the gastrocnemius and plantaris in maintaining muscle mass, as they were significantly less than control by 15%[45]. Hindlimb unweighting was further determined as a cause for reduced muscle mass in adult rats[47]. Soleus muscle mass was significantly reduced in hindlimb unloaded growing rats compared to control rats after 17 days of unloading[46]. This effect was reversed after a 28-day reambulation period. The authors noted that during hindlimb unloading, the ankle was plantarflexed, which caused shortening of the soleus and reduced muscle mass[54]. The mechanism of unloading largely affects muscle properties. If the limb is held in place by a cast, it could be immobilized in a shortened position, which has been shown to have detrimental effects on muscle. In a model in which the unloaded limbs are exposed, they can be held at a natural, optimal position, which may not have as much of an effect of muscle.

Our forelimb suspension system differs from hindlimb suspension systems in that, although the suspended limbs are non-weight bearing, they still experience some non-weight-bearing loading and muscle activity during daily grooming and eating activities. Because muscle mass and optimal muscle length were, for the most part, similar between the suspension and control groups, this small amount of loading seems sufficient to stimulate normal forelimb muscle growth. However, our forearm amputation group experienced both reduced weight bearing and reduced limb use following amputation and were unable to walk on or groom with the amputated limb normally. The affected limb served only as an occasional weight-bearing stabilizer, and forelimb muscle use during these daily activities was greatly reduced. Therefore, the reduced muscle mass observed in this group, compared both to the contralateral limb and to the suspension and control groups, may result from limb disuse rather than direct unloading of the muscles.

Limitations

Both male and female rats were compared together, and sex differences were not considered. Young (3-month old) male rats have shown to display greater reduction in total body mass compared to control rats over the hindlimb unloading period, while females did not[48]. The amputation group comprised of 3 male rats, whereas the other groups had at least one female, which could help explain why the amputation group displayed greater significance. The forelimb suspension group was sacrificed one week later than the forelimb amputation and control groups to accommodate the four male rats that were removed from the suspension system for a brief 4-day period due to elevated stress, as indicated by lesions underneath the harness and porphyrin discharge around the nose and eyes[36]. The removal occurred during the third week of unloading, but the rats progressed normally after the wounds healed. In the future, an additional layer of

345 breathable fabric should be placed between the harness and rat to reduce the amount of chaffing
346 and discomfort over the long unloading period. The suspension system, while removing weight
347 bearing from the forelimbs, did not completely eliminate loading, as the animals were able to
348 continue normal grooming and feeding activities, as noted above. With forearm amputation,
349 because the affected limb experienced reduced weight bearing and overall use, the contralateral
350 limb likely was loaded more throughout the study, potentially augmenting the side differences
351 observed. Nevertheless, similar muscle changes were observed for the affected limb compared to
352 the normally loaded limb of the control group.
353
354 **Conclusions**
355 Altered loading affected upper forelimb muscle mass and optimal muscle length, primarily
356 in the biceps and triceps muscles of the forearm amputation group. The forelimb suspension group
357 did not experience marked differences from the control group, showing that this unloading
358 paradigm did not negatively impact muscle growth and function, as in the forearm amputation
359 group. Our results suggest that even limited amounts of forelimb loading during non-weight-
360 bearing activities offset the unloading detriments observed in hindlimb unloading models, and
361 general limb use is more important for muscle growth than weight bearing. The muscle responses
362 in the amputation group more closely mimicked those results seen in nerve injury groups, making
363 this a more suitable model to assess isolated muscle effects due to forelimb unloading.

References

1. Arvind V, Huang AH. 2017. Mechanobiology of limb musculoskeletal development. Ann N Y Acad Sci 1409(1):18–32.
2. Felsenthal N, Zelzer E. 2017. Mechanical regulation of musculoskeletal system development. Development 144(23):4271–4283.
3. Qin Y-X, Hu M. 2014. Mechanotransduction in Musculoskeletal Tissue Regeneration: Effects of Fluid Flow, Loading, and Cellular-Molecular Pathways. BioMed Research International [cited 2019 Feb 20] Available from: https://www.hindawi.com/journals/bmri/2014/863421/.
4. Shwartz Y, Blitz E, Zelzer E. 2013. One load to rule them all: Mechanical control of the musculoskeletal system in development and aging. Differentiation 86(3):104–111.
5. Klein L, Heiple KG, Stromberg BV. 1983. Comparison of growth-induced resorption and denervation-induced resorption on the release of [3H]tetracycline, 45calcium, and [3H]collagen from whole bones of growing rats. J. Orthop. Res. 1(1):50–56.
6. Laib A, Barou O, Vico L, et al. 2000. 3D micro-computed tomography of trabecular and cortical bone architecture with application to a rat model of immobilisation osteoporosis. Med. Biol. Eng. Comput. 38(3):326–332.
7. Warner SE, Sanford DA, Becker BA, et al. 2006. Botox induced muscle paralysis rapidly degrades bone. Bone 38(2):257–264.
8. Bouvard B, Mabilleau G, Legrand E, et al. 2012. Micro and macroarchitectural changes at the tibia after botulinum toxin injection in the growing rat. Bone 50(4):858–864.
9. Tascher G, Brioche T, Maes P, et al. 2017. Proteome-wide Adaptations of Mouse Skeletal Muscles during a Full Month in Space. J. Proteome Res. 16(7):2623–2638.

10. Yu Q, Morales M, Li N, et al. 2018. Skeletal, cardiac, and respiratory muscle function and histopathology in the P448Lneo− mouse model of FKRP-deficient muscular dystrophy. Skelet Muscle 8 [cited 2018 Nov 7] Available from: https://www.ncbi.nlm.nih.gov/pmc/articles/PMC5889611/.

11. Heinemeier KM, Olesen JL, Haddad F, et al. 2009. Effect of unloading followed by reloading on expression of collagen and related growth factors in rat tendon and muscle. J. Appl. Physiol. 106(1):178–186.

12. Ohira Y, Kawano F, Wang XD, et al. 2006. Irreversible morphological changes in leg bone following chronic gravitational unloading of growing rats. Life Sciences 79(7):686–694.

13. Globus RK, Morey-Holton E. 2016. Hindlimb unloading: rodent analog for microgravity. Journal of Applied Physiology 120(10):1196–1206.

14. Abicht A, Müller J, Lochmüller H. 1993. Congenital Myasthenic Syndromes. In: Adam MP, Ardinger HH, Pagon RA, et al., editors. GeneReviews®. Seattle (WA): University of Washington, Seattle [cited 2018 Nov 8] Available from: http://www.ncbi.nlm.nih.gov/books/NBK1168/.

15. Sparks SE, Quijano-Roy S, Harper A, et al. 1993. Congenital Muscular Dystrophy Overview. In: Adam MP, Ardinger HH, Pagon RA, et al., editors. GeneReviews®. Seattle (WA): University of Washington, Seattle [cited 2018 Nov 8] Available from: http://www.ncbi.nlm.nih.gov/books/NBK1291/.

16. Stavsky M, Mor O, Mastrolia SA, et al. 2017. Cerebral Palsy—Trends in Epidemiology and Recent Development in Prenatal Mechanisms of Disease, Treatment, and Prevention. Front Pediatr 5 [cited 2018 Nov 8] Available from: https://www.ncbi.nlm.nih.gov/pmc/articles/PMC5304407/.

410 17. Chauhan SP, Blackwell SB, Ananth CV. 2014. Neonatal brachial plexus palsy: incidence,
411 prevalence, and temporal trends. Semin. Perinatol. 38(4):210–218.
412 18. Soldado F, Fontecha CG, Marotta M, et al. 2014. The role of muscle imbalance in the
413 pathogenesis of shoulder contracture after neonatal brachial plexus palsy: a study in a rat
414 model. J Shoulder Elbow Surg 23(7):1003–1009.
415 19. Wang B, Chen L, Liu B, et al. 2012. Differentiation of endogenous neural stem cells in adult
416 versus neonatal rats after brachial plexus root avulsion injury. Neural Regen Res 7(23):1786–
417 1790.
418 20. Wang Z-Q, Xiu D-H, Liu G-F, Jiang J-L. 2018. Overexpression of Neuregulin-1 (NRG-1)
419 Gene Contributes to Surgical Repair of Brachial Plexus Injury After Contralateral C7 Nerve
420 Root Transfer in Rats. Med. Sci. Monit. 24:5779–5787.
421 21. Rodrigues M, Echigoya Y, Fukada S, Yokota T. [date unknown]. Current Translational
422 Research and Murine Models For Duchenne Muscular Dystrophy. J Neuromuscul Dis
423 3(1):29–48.
424 22. Dowling JJ, D. Gonorazky H, Cohn RD, Campbell C. 2018. Treating pediatric neuromuscular
425 disorders: The future is now. Am J Med Genet A 176(4):804–841.
426 23. Clowry GJ, Basuodan R, Chan F. 2014. What are the Best Animal Models for Testing Early
427 Intervention in Cerebral Palsy? Front Neurol 5 [cited 2018 Nov 8] Available from:
428 https://www.ncbi.nlm.nih.gov/pmc/articles/PMC4255621/.
429 24. Feather-Schussler DN, Ferguson TS. 2016. A Battery of Motor Tests in a Neonatal Mouse
430 Model of Cerebral Palsy. J Vis Exp (117) [cited 2018 Nov 8] Available from:
431 https://www.ncbi.nlm.nih.gov/pmc/articles/PMC5226120/.

25. Tan J, Zheng X, Zhang S, et al. 2014. Response of the sensorimotor cortex of cerebral palsy rats receiving transplantation of vascular endothelial growth factor 165-transfected neural stem cells. Neural Regen Res 9(19):1763–1769.

26. Ban J, Phillips WD. 2015. Mouse models of myasthenia gravis. Curr. Pharm. Des. 21(18):2468–2486.

27. [Date unknown]. Fatigue and Muscle Atrophy in a Mouse Model of Myasthenia Gravis Is Paralleled by Loss of Sarcolemmal nNOS. [cited 2018 Nov 8] Available from: https://journals.plos.org/plosone/article?id=10.1371/journal.pone.0044148.

28. Mantegazza R, Cordiglieri C, Consonni A, Baggi F. 2016. Animal models of myasthenia gravis: utility and limitations. Int J Gen Med 9:53–64.

29. Lee S, Shin J, Hong Y, et al. 2012. Beneficial effects of melatonin on stroke-induced muscle atrophy in focal cerebral ischemic rats. Lab Anim Res 28(1):47–54.

30. Biering-Sørensen B, Kristensen IB, Kjaer M, Biering-Sørensen F. 2009. Muscle after spinal cord injury. Muscle Nerve 40(4):499–519.

31. Borschmann KN, Rewell SS, Iuliano S, et al. 2017. Reduced bone formation markers, and altered trabecular and cortical bone mineral densities of non-paretic femurs observed in rats with ischemic stroke: A randomized controlled pilot study. PLoS ONE 12(3):e0172889.

32. Norlin R, Hoe-Hansen C, Oquist G, Hildebrand C. 1994. Shoulder region of the rat: anatomy and fiber composition of some suprascapular nerve branches. Anat. Rec. 239(3):332–342.

33. Soslowsky LJ, Carpenter JE, DeBano CM, et al. 1996. Development and use of an animal model for investigations on rotator cuff disease. J Shoulder Elbow Surg 5(5):383–392.

34. Quinn R. 2005. Comparing rat's to human's age: how old is my rat in people years? Nutrition 21(6):775–777.

455 35. Morey-Holton ER, Globus RK. 2002. Hindlimb unloading rodent model: technical aspects.
456 J. Appl. Physiol. 92(4):1367–1377.
457 36. Wagner EB, Granzella NP, Saito H, et al. 2010. Partial weight suspension: a novel murine
458 model for investigating adaptation to reduced musculoskeletal loading. J. Appl. Physiol.
459 109(2):350–357.
460 37. van den Brand R, Heutschi J, Barraud Q, et al. 2012. Restoring voluntary control of
461 locomotion after paralyzing spinal cord injury. Science 336(6085):1182–1185.
462 38. Tushak S, Tamburro M. 2018. Development of a Rat Forelimb Unloading Model to
463 Understand Mechanical Influences on Postnatal Shoulder Development. 2018 NCUR 0(0)
464 [cited 2018 Nov 8] Available from:
465 http://www.ncurproceedings.org/ojs/index.php/NCUR2018/article/view/2673.
466 39. Crouch DL, Hutchinson ID, Plate JF, et al. 2015. Biomechanical Basis of Shoulder Osseous
467 Deformity and Contracture in a Rat Model of Brachial Plexus Birth Palsy. J Bone Joint Surg
468 Am 97(15):1264–1271.
469 40. Ward SR, Sarver JJ, Eng CM, et al. 2010. Plasticity of Muscle Architecture After Acute
470 Supraspinatus Tear. J Orthop Sports Phys Ther 40(11):729–735.
471 41. Toursel T, Stevens L, Granzier H, Mounier Y. 2002. Passive tension of rat skeletal soleus
472 muscle fibers: effects of unloading conditions. Journal of Applied Physiology 92(4):1465–
473 1472.
474 42. Booth CM, Cortina-Borja MJ, Theologis TN. 2001. Collagen accumulation in muscles of
475 children with cerebral palsy and correlation with severity of spasticity. Dev Med Child Neurol
476 43(5):314–320.

43. Nikolaou S, Liangjun H, Tuttle LJ, et al. 2014. Contribution of denervated muscle to contractures after neonatal brachial plexus injury: not just muscle fibrosis. Muscle Nerve 49(3):398–404.

44. Adams GR, Haddad F, Bodell PW, Tran PD, Baldwin KM. 2007. Combined isometric, concentric, and eccentric resistance exercise prevents unloading-induced muscle atrophy in rats. J Appl Physiol 103, 1644-54.

45. Hurst JE, Fitts RH. 2003. Hindlimb unloading-induced muscle atrophy and loss of function: protective effect of isometric exercise. J Appl Physiol 95: 1405-1417.

46. Ohira Y, Tanaka T, Yoshinaga T, Kawano F, Nomura T, Nonaka I, Allen DL, Roy RR, Edgerton VR. 2001. Ontogenetic, gravity-dependent development of rat soleus muscle. Am J Physiol Cell Physiol 280(4): C1008-16.

47. Brown M, Fisher JS, Salsich G. 1999. Stiffness and muscle function with age and reduced muscle use. J. Orthop. Res. 17, 409–414.

48. Deschenes MR, Adan MA, Kapral MC, Kressin KA, Leathrum CM, Seo A, Li S, Schaffrey EC. 2018. Neuromuscular Adaptability of Male and Female Rats to Muscle Unloading. J Neurosci Res 96(2): 284-96.

49. Zajac FE. Muscle and tendon: Properties, models, scaling, and application to biomechanics 303 and motor control. Crit Rev Biomed Eng. 1989;17(4):359.

50. Dixit NN, McCormick C, Warren E, Cole JH, Saul K (2019) Preganglionic and postganglionic brachial plexus injury effects on shoulder muscle growth. J Hand Surg .

51. Hultgren T, Einarsson F, Runesson E, Hemlin C, Friden J, Ljung BO. 2010. Structural characteristics of the subscapularis muscle in children with medial rotation contracture of the shoulder after obstetric brachial plexus injury. J Hand Surg Eur 35(1): 23-28.

500 52. Gutmann E (ed.). 1962. The Denervated Muscle.

501 53. Goldspink DF. 1976. The Effects of Denervation on Protein Turnover of Rat Skeletal Muscle.

502 Biochem J 156, 71-80.

503 54. Goldspink DF. 1977. The influence of immobilization and stretch on protein turnover of rat

504 skeletal muscle. J Physiol 264, 267-282.

505 55. Kasper CE, Xun L. 2000. Expression of Titin in Skeletal Muscle Varies with Hind-Limb

506 Unloading. Biological Research for Nursing 2(2): 107-115.

507 **Figures**

508

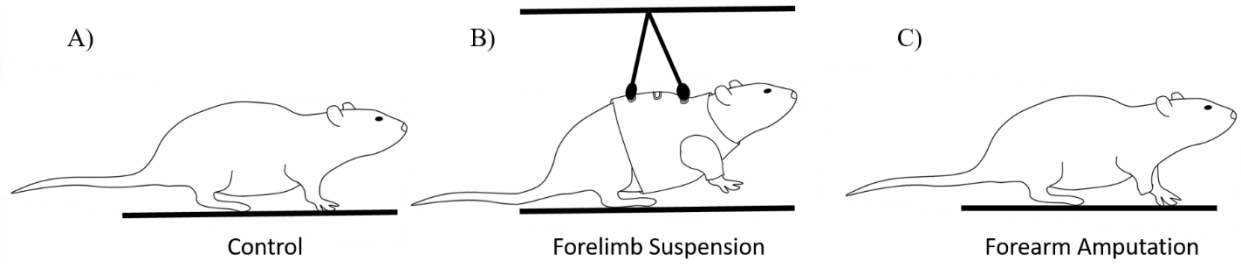

509

510 **Figure 1.** The study design included a A) control group (both forelimbs unaffected by unloading;
511 right forelimb examined) and two unloading paradigms, B) forelimb suspension (both forelimbs
512 affected) and C) forearm amputation (right forelimb affected, left forelimb unaffected).

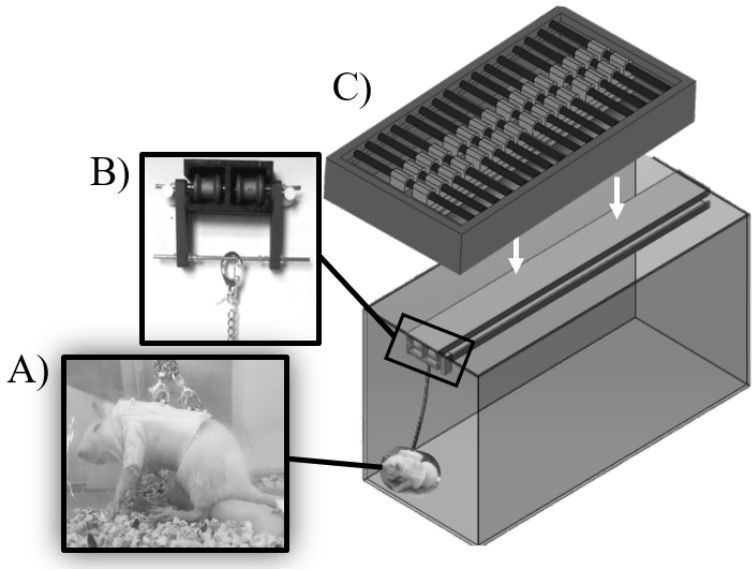

Figure 2. Custom forelimb suspension apparatus. A) Commercial harness sized to the growing rat was tethered at two points using swivel hooks and adjustable chain and attached to the B) 3D printed I-beam track system with low-friction wheels. C) Sixteen wooden dowels were inserted into loops printed atop the track system to secure it within the lid.

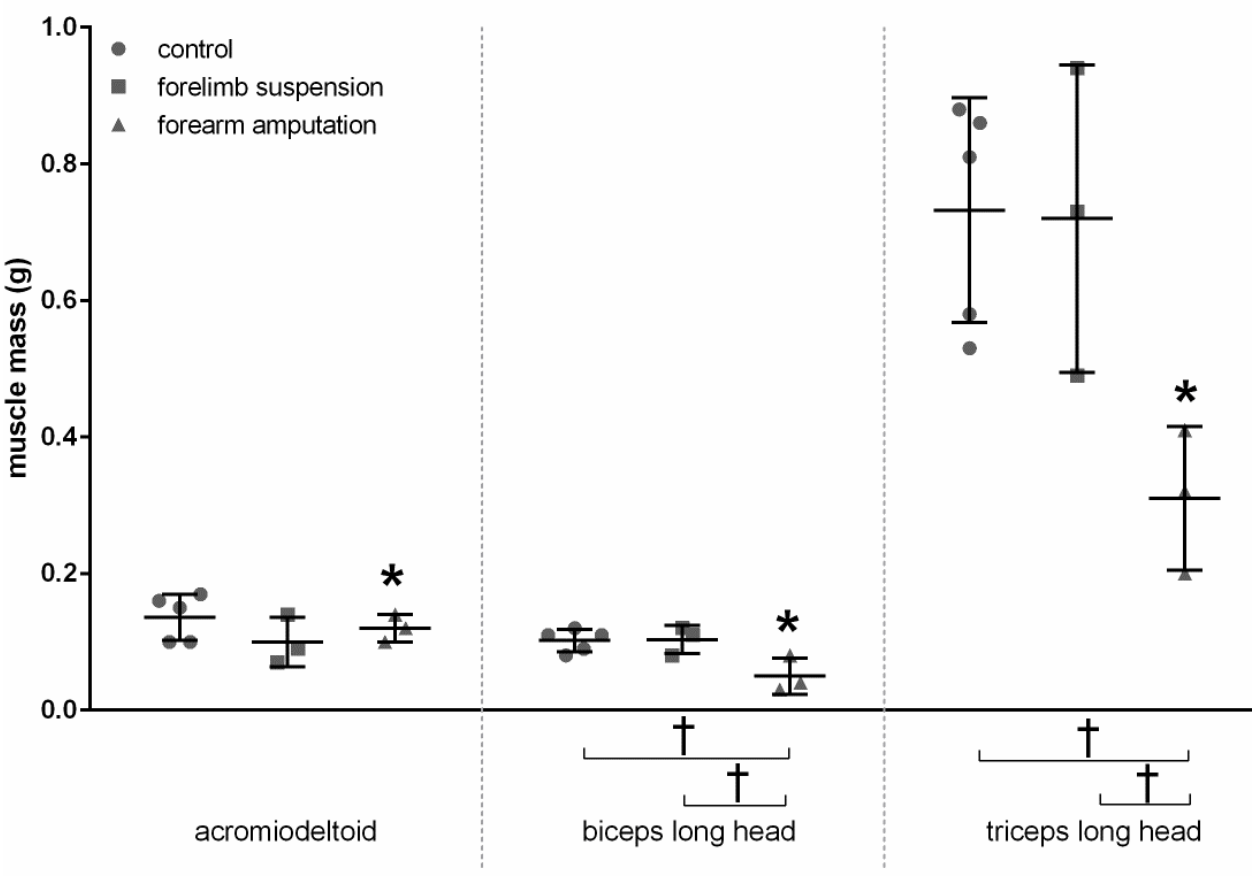

Figure 3. Muscle mass of forelimb muscles showing significant side-to-side differences (forearm amputation only) and group differences (control, forelimb suspension, forearm amputation). Mean ± standard deviation. *$p < 0.05$ for right vs. left limb. #$p < 0.1$ (trend) for right vs. left limb. †$p < 0.05$ for group comparisons.

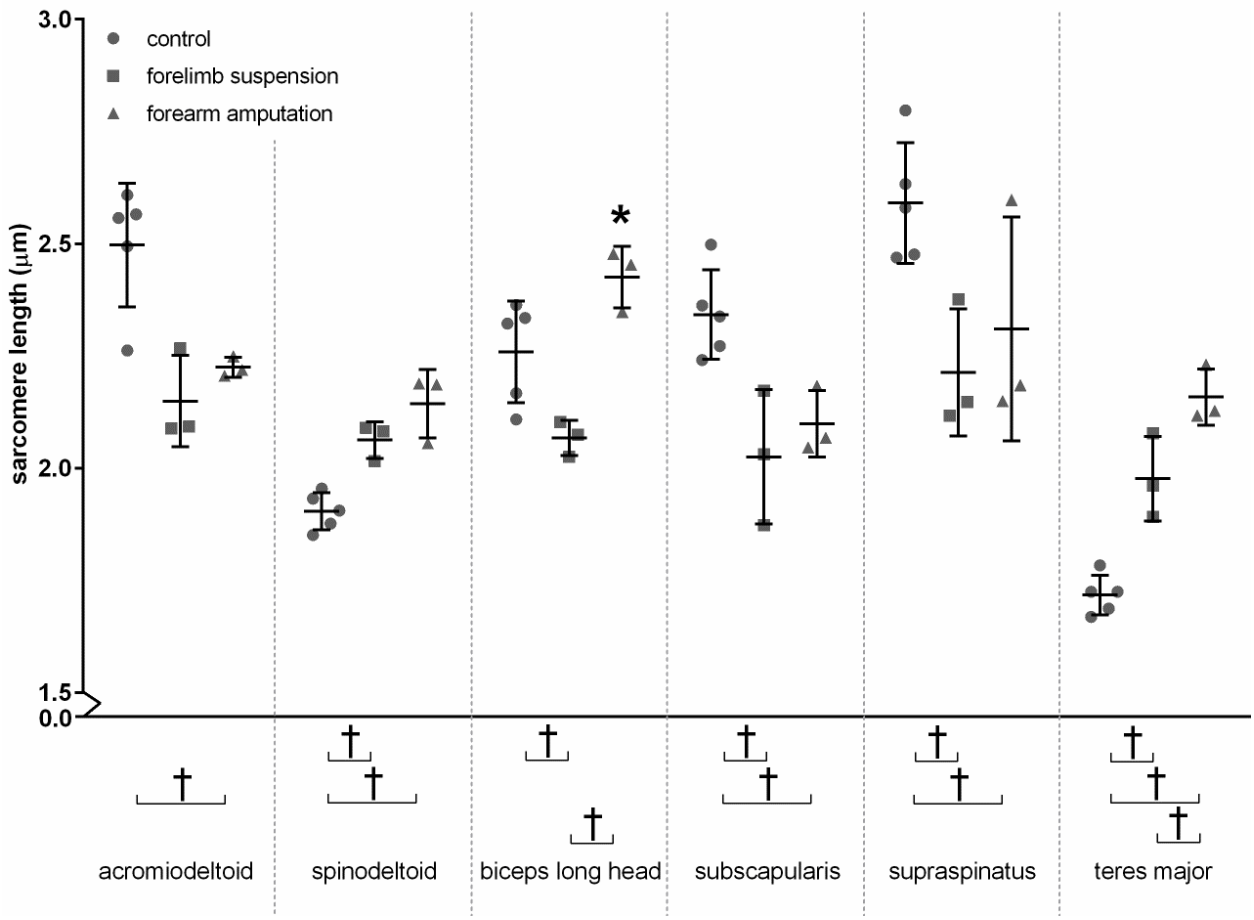

Figure 4. Muscle sarcomere lengths showing significant side-to-side differences (forearm amputation only) and group differences (control, forelimb suspension, forearm amputation). Mean ± standard deviation. *$p < 0.05$ for right vs. left limb. #$p < 0.1$ (trend) for right vs. left limb. †$p < 0.05$ for group comparisons. ‡$p < 0.1$ (trend) for group comparisons.

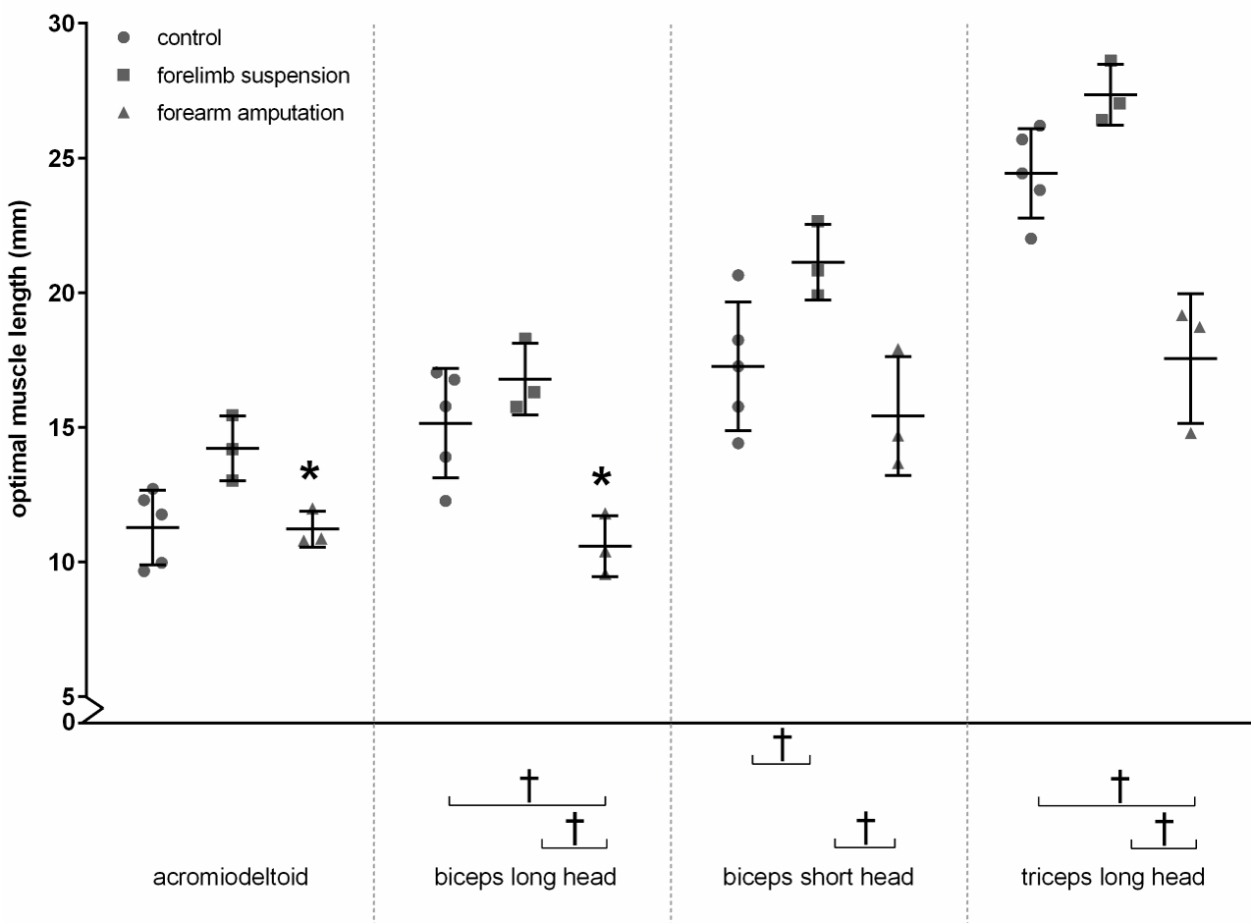

Figure 5. Optimal muscle lengths showing significant side-to-side differences (forearm amputation only) and group differences (control, forelimb suspension, forearm amputation). Mean ± standard deviation. *$p < 0.05$ for right vs. left limb. #$p < 0.1$ (trend) for right vs. left limb. †$p < 0.05$ for group comparisons. ‡$p < 0.1$ (trend) for group comparisons.

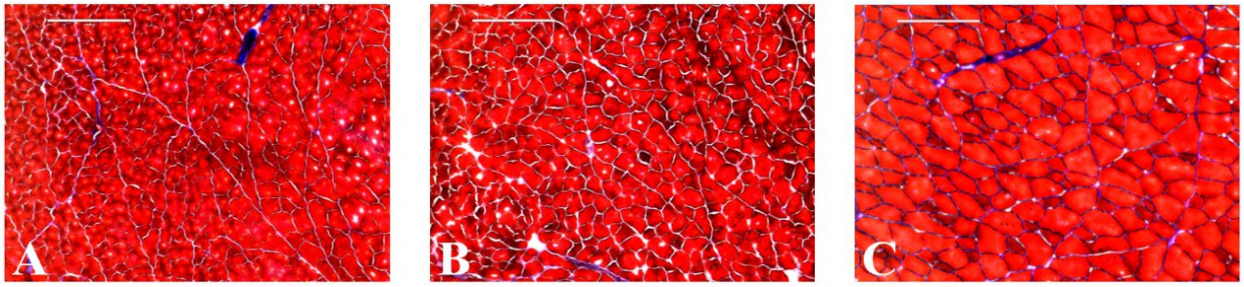

Figure 6. Longitudinal section of biceps long head muscle in A) control, B) forelimb suspension, and C) forearm amputation groups, stained to assess collagen area (blue) as a percentage of muscle tissue area (red). Scale bars = 200 μm.

Tables

Table 1. Muscle mass, sarcomere length, and optimal muscle length for the control (left forelimb), forelimb suspension (right forelimb), and forearm amputation (both forelimbs) groups. Mean ± standard deviation.

	control			**forelimb suspension**		
	left (unaffected)			right (affected)		
	mass (g)	sarcomere length (μm)	optimal length (mm)	mass (g)	sarcomere length (μm)	optimal length (mm)
pectoralis major	0.34 ± 0.08[a]	2.33 ± 0.27	19.4 ± 2.1	0.23 ± 0.03	1.92 ± 0.08	22.2 ± 3.3
acromiodeltoid	0.14 ± 0.03	2.49 ± 0.14	11.3 ± 1.4	0.10 ± 0.03	2.15 ± 0.10	14.2 ± 1.2
spinodeltoid	0.14 ± 0.03	1.90 ± 0.04	20.1 ± 1.8	0.12 ± 0.05	2.06 ± 0.04	25.0 ± 2.4
biceps long head	0.10 ± 0.02	2.26 ± 0.11	15.2 ± 2.0	0.10 ± 0.02	2.07 ± 0.04	16.8 ± 1.3
biceps short head	0.01 ± 0.01	2.09 ± 0.21	17.3 ± 2.4	0.04 ± 0.02	1.95 ± 0.06	21.1 ± 1.4
subscapularis	0.27 ± 0.05	2.34 ± 0.10	18.2 ± 3.0	0.19 ± 0.06	2.03 ± 0.15	21.6 ± 0.6
supraspinatus	0.21 ± 0.06	2.59 ± 0.13	20.2 ± 2.2	0.20 ± 0.05	2.21 ± 0.14	23.7 ± 1.0
infraspinatus	0.22 ± 0.05	2.37 ± 0.10	22.1 ± 2.6	0.19 ± 0.02	2.22 ± 0.05	24.0 ± 2.0
teres major	0.21 ± 0.05	1.72 ± 0.04	24.5 ± 2.8	0.21 ± 0.05	1.98 ± 0.09	25.0 ± 0.9
triceps long head	0.73 ± 0.16	1.98 ± 0.13	24.4 ± 1.7	0.72 ± 0.23	1.89 ± 0.03	27.3 ± 1.1

[a] Pectoralis major muscle mass was lower in right vs. left limb, likely due to sham surgery in previous study.

	forearm amputation					
	left (unaffected)			right (affected)		
	mass (g)	sarcomere length (μm)	optimal length (mm)	mass (g)	sarcomere length (μm)	optimal length (mm)
pectoralis major	0.27 ± 0.15	2.07 ± 0.08	31.5 ± 10.1	0.26 ± 0.07	2.21 ± 0.07	23.4 ± 2.5
acromiodeltoid	0.15 ± 0.03	2.18 ± 0.03	15.4 ± 0.8	0.12 ± 0.02*	2.23 ± 0.02	11.2 ± 0.7*
spinodeltoid	0.13 ± 0.03	2.19 ± 0.01	23.7 ± 2.7	0.13 ± 0.01	2.14 ± 0.08	16.8 ± 6.9
biceps long head	0.11 ± 0.04	2.06 ± 0.08*	17.5 ± 1.0	0.05 ± 0.03*	2.43 ± 0.07	10.6 ± 1.1*
biceps short head	0.02 ± 0.01	1.99 ± 0.01	19.1 ± 0.2	0.03 ± 0.01	2.22 ± 0.13	15.4 ± 2.2
subscapularis	0.20 ± 0.10	2.14 ± 0.09	23.9 ± 2.8	0.28 ± 0.06	2.10 ± 0.07	22.3 ± 0.9
supraspinatus	0.24 ± 0.11	2.33 ± 0.11	24.2 ± 1.9	0.14 ± 0.05	2.31 ± 0.25	21.6 ± 3.5
infraspinatus	0.22 ± 0.03	2.37 ± 0.13	25.0 ± 2.8	0.17 ± 0.03	2.30 ± 0.05	21.1 ± 1.7
teres major	0.23 ± 0.04	2.05 ± 0.05	24.9 ± 1.3	0.22 ± 0.06	2.16 ± 0.06	22.6 ± 0.7
triceps long head	0.71 ± 0.18	2.03 ± 0.05	24.6 ± 2.7	0.31 ± 0.11*	2.07 ± 0.10	17.6 ± 2.4

*$p < 0.05$ for smaller value vs. contralateral limb.

546 **Table 2.** Percent collagen content for the control (left forelimb), forelimb suspension (right
547 forelimb), and forearm amputation (right forelimb) groups. Mean ± standard deviation.

	control	forelimb suspension	forearm amputation
biceps long head	5.9 ± 1.3	5.9 ± 0.8[a]	5.9 ± 0.0[b]
biceps short head	6.0 ± 1.3	4.7 ± 0.3[a]	7.9 ± 0.0[b]
upper subscapularis	5.8 ± 2.0	4.1 ± 0.5	5.5 ± 1.7
lower subscapularis	8.1 ± 2.0[a]	4.3 ± 1.1	4.4 ± 1.0

[a]Not all specimens could to be imaged.
[b]Not all specimens could be sectioned.

548